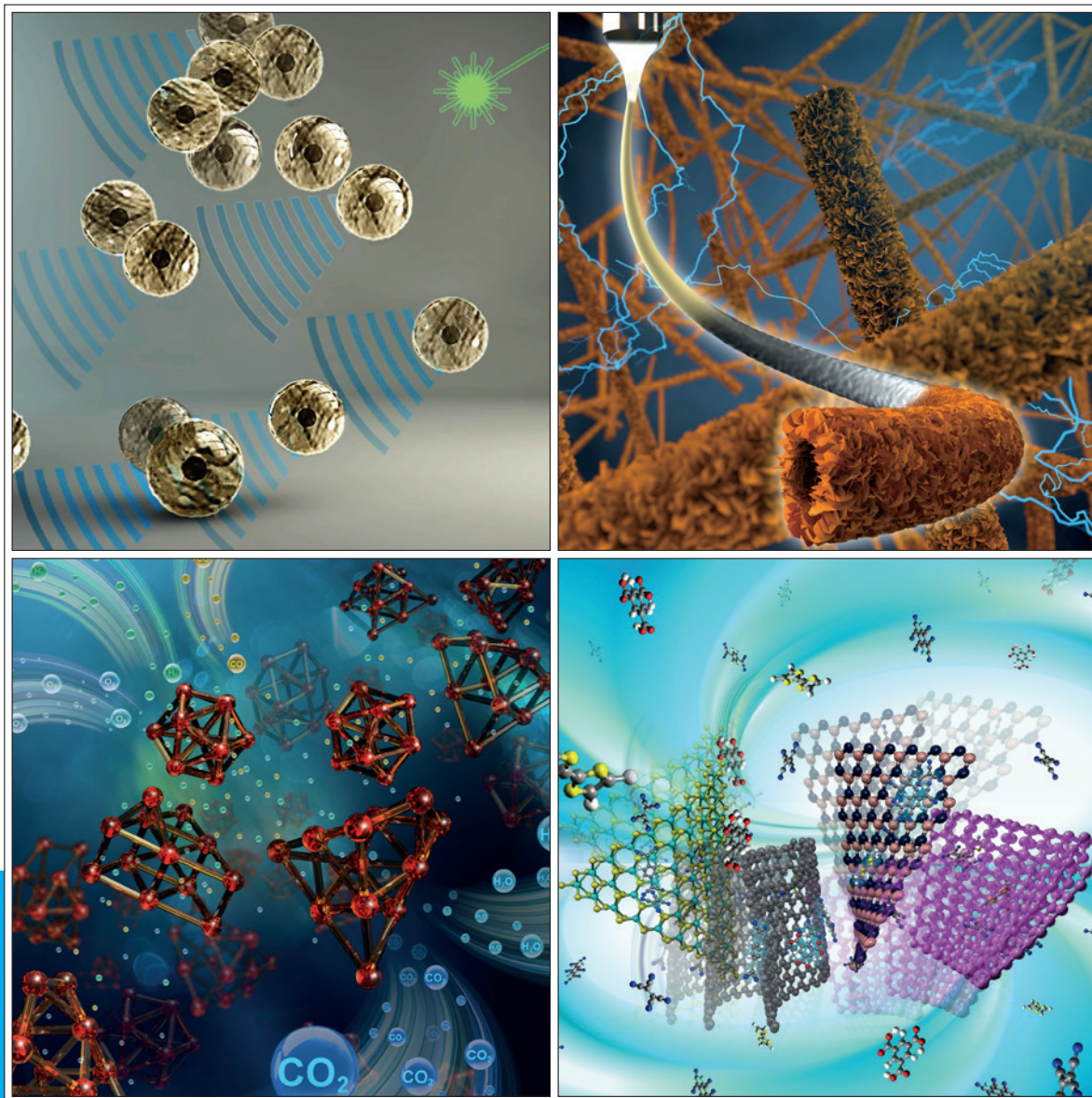


CHEM**NANO**MAT

CHEMISTRY OF NANOMATERIALS FOR ENERGY, BIOLOGY AND MORE

www.chemnanomat.org



A Journal of



REPRINT

WILEY-VCH

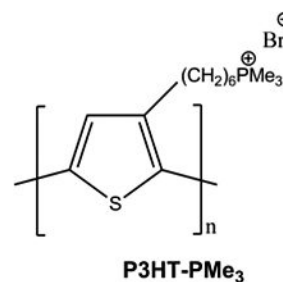
Supramolecular Self-Assembly of DNA with a Cationic Polythiophene: From Polyplexes to Fibers

Maxime Leclercq,^[a] Jenifer Rubio-Magnieto,^[a, e] Danahe Mohammed,^[b] Sylvain Gabriele,^[b] Laurent Leclercq,^[c] Hervé Cottet,^{*[c]} Sébastien Richeter,^[d] Sébastien Clément,^{*[d]} and Mathieu Surin^{*[a]}

Abstract: Cationic polythiophenes constitute an interesting class of polymers for prospective applications in imaging, gene delivery and biosensing, as they combine solubility in aqueous media and have sensitive optical properties for the detection of biomolecules such as DNA. Here, we study the supramolecular self-assembly of poly[3-(6'-(trimethylphosphonium)hexyl)thiophene-2,5-diyl] (**P3HT-PMe₃**) with different types of DNA such as single-stranded oligonucleotides or long genomic DNA. Self-assembly in buffered aqueous solution yields polyplexes (polymer/DNA complexes) with hydrodynamic radii ranging from 7 nm to around 25 nm, as observed by Taylor Dispersion Analysis. In these polyplexes, the achiral polymer presents chiroptical signals induced by supramolecular organization along chiral DNA. When the solution of long DNA/**P3HT-PMe₃** is deposited on surfaces, tens of μm -long fibers are formed by condensation of DNA and compaction of the polyplexes, as evidenced by microscopy techniques.

interactions between biomolecules and synthetic (macro)molecules enable the self-assembly of functional hybrid materials, often referred to as biohybrid materials.^[2] Notably, hybrid supramolecular nanostructures combining DNA and synthetic polymers are of high current interest for developing a wide range of applications, notably in gene delivery, sensing, and hydrogels.^[3] In this frame, there has been many studies on the design of cationic π -conjugated oligomers or polymers that interact with DNA mainly *via* electrostatic interactions, with applications in the fields of DNA concentration assays and DNA hybridization detection.^[4] In this frame, cationic polythiophenes (CPTs) are an interesting class of π -conjugated nanomaterials for binding DNA.^[4c, 5] Recently, CPTs were successfully used for DNA delivery into tumour cells,^[6] for improving transgene efficiency of polypeptide-based gene carriers,^[7] or for the regulation of gene expression through a photoinduced unwinding of plasmid DNA when it is assembled with CPTs.^[8] In this context, some of us designed poly[3-(6'-(trimethylphosphonium)hexyl)thiophene-2,5-diyl] (**P3HT-PMe₃**, see Scheme 1) that

Supramolecular self-assembly has been thoroughly exploited to achieve well-defined nanostructures for prospective applications in biomedical fields, for instance in regenerative medicine, biosensing, and medical imaging.^[1] Fine control over the



Scheme 1. Chemical structure of the cationic poly[3-(6'-(trimethylphosphonium)hexyl)thiophene-2,5-diyl], **P3HT-PMe₃**.

[a] M. Leclercq, Dr. J. Rubio-Magnieto, Prof. M. Surin
Laboratory for Chemistry of Novel Materials
Center for Innovation in Materials and Polymers
University of Mons – UMONS, 20 Place du Parc, B-7000 Mons, Belgium
E-mail: mathieu.surin@umons.ac.be

[b] Dr. D. Mohammed, Prof. S. Gabriele
Mechanobiology & Soft Matter Group
Laboratoire Interfaces et Fluides Complexes
Center for Innovation in Materials and Polymers
University of Mons – UMONS, 20 Place du Parc, B-7000 Mons, Belgium

[c] Dr. L. Leclercq, Prof. H. Cottet
Institut des Biomolécules Max Mousseron (IBMM), Université de Montpellier,
CNRS, ENSCM, Montpellier, France
E-mail: herve.cottet@umontpellier.fr

[d] Dr. S. Richeter, Prof. S. Clément
Institut Charles Gerhardt (ICGM), UMR 5253 CNRS-ENSCM-UM, Université de
Montpellier – CC1701, Place Eugène Bataillon, F-34095 Montpellier Cedex 05,
France
E-mail: sebastien.clement1@umontpellier.fr

[e] Dr. J. Rubio-Magnieto
Current address: Bioinspired Supramolecular Chemistry and Materials Group
Departament de Química Inorgànica i Orgànica Universitat Jaume I, Avda
Sos Baynat s/n, E-12071, Castelló, Spain

Supporting information for this article is available on the WWW under
<https://doi.org/10.1002/cnma.201900022>

showed DNA sequence-dependent chiroptical signals in the spectral range of the polythiophene when mixed with oligonucleotides (ODNs) in solution.^[9] Together with the fluorescence of the polymer, the (chir)optical signals were exploited to probe the hybridization between complementary oligonucleotides.^[10]

Here, we report on the supramolecular structures formed by the complexation of **P3HT-PMe₃** and DNAs of various lengths. We demonstrate that, in aqueous buffered solutions, the self-assembly of **P3HT-PMe₃** and DNA leads to the formation of polyplexes (*i.e.* polymer/DNA complexes) with sizes ranging from a few nm for the shortest DNA to around 25 nm for long DNA, which is typically the range for polyplexes currently used for cell transfection.^[11] We describe the evolution of the

Table 1. Polyplex average hydrodynamic radii (R_h), average number of ligands per DNA chain \bar{n} and charge ratio stoichiometry n^+/n^- in the polyplex obtained by TDA for the different systems based on P3HT-PMe ₃ polycation.					
Polyplex (ODN/ P3HT-PMe ₃)	N/P ratio	R_h (nm)	% of free P3HT-PMe ₃	\bar{n}	n^+/n^-
sDNA/P3HT-PMe ₃	12	25.5 ± 1.8	56 ± 1	341	5.3
dT ₂₀ /P3HT-PMe ₃	1	7.2 ± 0.6	4 ± 1	0.3	1.0
dT ₂₀ /P3HT-PMe ₃	10	7.4 ± 0.5	50 ± 1	1.6	5.0

chiroptical properties going from solution to the solid-state, together with a morphological study on the hierarchical self-assembly of long DNA with P3HT-PMe₃ into fiber-like structures extending from μm to hundreds μm in length.

Taylor Dispersion Analysis

Taylor dispersion analysis (TDA) is an absolute method (no calibration required) giving access to diffusion coefficient (or hydrodynamic radius) of any solute in the range of angstrom up to sub-micron.^[12] TDA is based on the analysis of band broadening under a laminar Poiseuille flow in an open tube. In the case of polycation mixtures, TDA give access to the weight-average hydrodynamic radius (R_h)^[13] of the polyplex, and to the free polycation concentration at equilibrium in the mixture.^[14] Figure 1 displays the taylorgram obtained for salmon DNA (sDNA) and P3HT-PMe₃ polyplex (N/P = 12 molar ratio) in frontal mode (continuous injection of the equilibrated mixture in the capillary). The taylorgram is the combination of two *erf* contributions (see experimental part): one pertaining to the free polycation in solution, and the other belonging to the polyplex. By fitting the taylorgram (see experimental part), the R_h of the free polycation chain was determined as 1.4 nm, which is of course much smaller than the polyplex (25.5 nm). Interestingly, the free polycation concentration at equilibrium in the mixture allows determining the average number of polycation chains

per DNA chain $\bar{n} = 341$ corresponding to a positive to negative charge ratio of $n^+/n^- = 5.3$, which means that the polyplex is highly positively charged. This finding is in agreement with the general rule recently enounced about the overall charge of polyelectrolyte complexes^[15] stating that if the polyelectrolyte of highest charge density between the two partners is introduced in excess in the mixture, the complex should have the same charge as this polyelectrolyte (here the polycation). Reversely, if the polyelectrolyte of highest charge density is introduced in default in the mixture, the complex should be stoichiometric (neutral, *i.e.* $n^+/n^- = 1$). Taylorgrams obtained for dT₂₀/P3HT-PMe₃ mixtures at different N/P ratios (1 and 10) are provided in the Supporting Information. The polyplex size for this system is about 7.3 nm for both N/P ratio. As expected from the rule previously enounced, the polyplex charge is stoichiometric in the case of N/P = 1 ratio, and highly positively charged ($n^+/n^- = 5$) for the N/P = 10 (see Table 1).

Chiroptical Properties of Polyplexes

UV-Vis absorption and Circular Dichroism (CD) spectroscopies were carried out on aqueous mixtures of P3HT-PMe₃ and DNA in various proportions in the same solution conditions than TDA studies (in TE buffer at pH 7.4). Figure 2 shows the UV-Vis and CD spectra of dT₂₀/P3HT-PMe₃ at a 1:1 DNA/polymer charge ratio. A large red-shift of the UV-Vis maximum absorption wavelength is observed when the polymer is mixed with oligonucleotide dT₂₀ ($\Delta\lambda_{\text{max}} = +28$ nm at 1:1 DNA/polymer charge ratio, see Figure 2a). Compared to the CD spectra of the pure compounds in the same conditions, two important effects are observed: (i) a decrease of CD signal in the wavelength range from 230–300 nm with respect to the pure DNA, and (ii) the appearance of a bisignate (+/–) induced CD signal (ICD) in the spectral range of P3HT-PMe₃ (from 400 nm to 600 nm). Indeed, ICD signals are important to probe the supramolecular chirality in self-assembled systems.^[16] The ICD reported here for dT₂₀/P3HT-PMe₃ is the signature of a right-handed helical conformation/ aggregation of the polythiophene chains in the supramolecular complexes.

When a long DNA (salmon DNA, sDNA) was mixed with P3HT-PMe₃ at a 1:1 charge ratio in aqueous buffered solution, the red-shift of the polymer main absorption band is also observed ($\Delta\lambda_{\text{max}} = +6$ nm, see Figure 3a) but much weaker than for mixtures with single-stranded DNAs (with dT₂₀, $\Delta\lambda_{\text{max}}$ is +28 nm). The CD signal in the range 230–300 nm slightly decreased and we did not observe any ICD signal in the range 400–600 nm (Figure 3b, blue line). However, when the charge

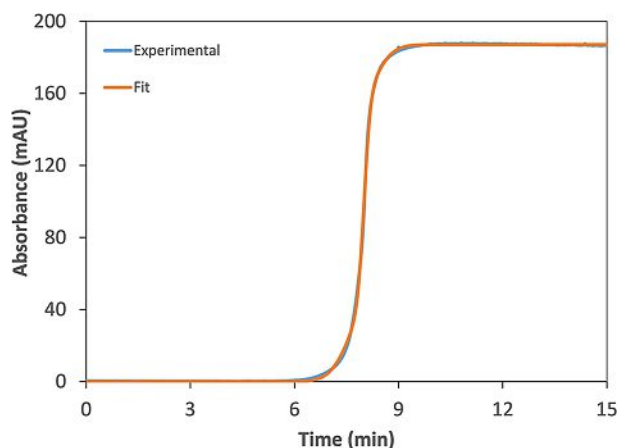


Figure 1. Taylorgram obtained for sDNA/P3HT-PMe₃ polyplex (N/P = 12) in frontal mode. Experimental conditions: PDADMAC-coated capillary 40 cm total length (30 cm to the UV detector) \times 50 μm i.d. Eluent: TE buffer. Mobilization pressure: 30 mbar. UV detection: 214 nm. Temperature: 25 °C. Erf fitting is displayed in red; experimental data are in blue.

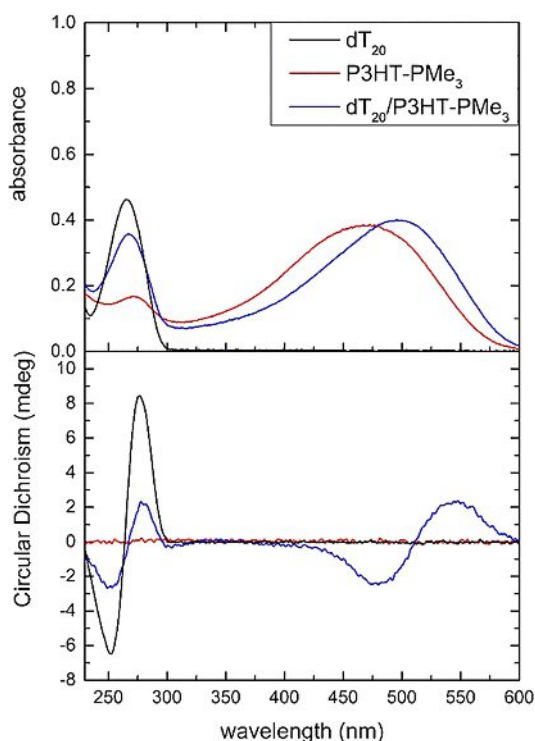


Figure 2. UV-Vis and CD spectra of dT_{20} (black line), $P3HT-PMe_3$ (red line) and $dT_{20}/P3HT-PMe_3$ complex (blue line) at a 1:1 DNA/polymer charge ratio.

ratio is higher, a weak ICD signal is observed (see Figure 3a), but much weaker than the ICD signals observed in mixtures with single-stranded oligonucleotides. The differences in the UV-Vis and CD spectra for mixtures with short oligonucleotides and long double-stranded DNA (salmon DNA) likely arises in the binding mechanisms: with single-stranded DNAs, besides electrostatic interactions, monomer-nucleobase interactions can occur (notably through π -type interactions), which planarize the π -conjugated backbone. In contrast, with double-stranded DNAs the bases are paired in the inner part of DNA, and thus, the monomer-nucleobase interactions are less likely.^[10]

The CD spectra of $sDNA/P3HT-PMe_3$ complex were measured in thin films deposited on quartz substrates, see Figure 3b (orange line). The CD spectrum is remarkably different than in solution: i) a CD signal is observed in the visible range, where only the polymer absorbs, and ii) in the range 230–300 nm, the CD signals (negative peak at 300 nm and a positive peak at 230 nm) are inverted compared to both pure $sDNA$ and $sDNA/P3HT-PMe_3$ mixture in solution. This reversed CD signal is the signature of a condensed and compacted DNA, as observed in so-called Polymer-Salt-Induced (PSI) aggregates.^[17]

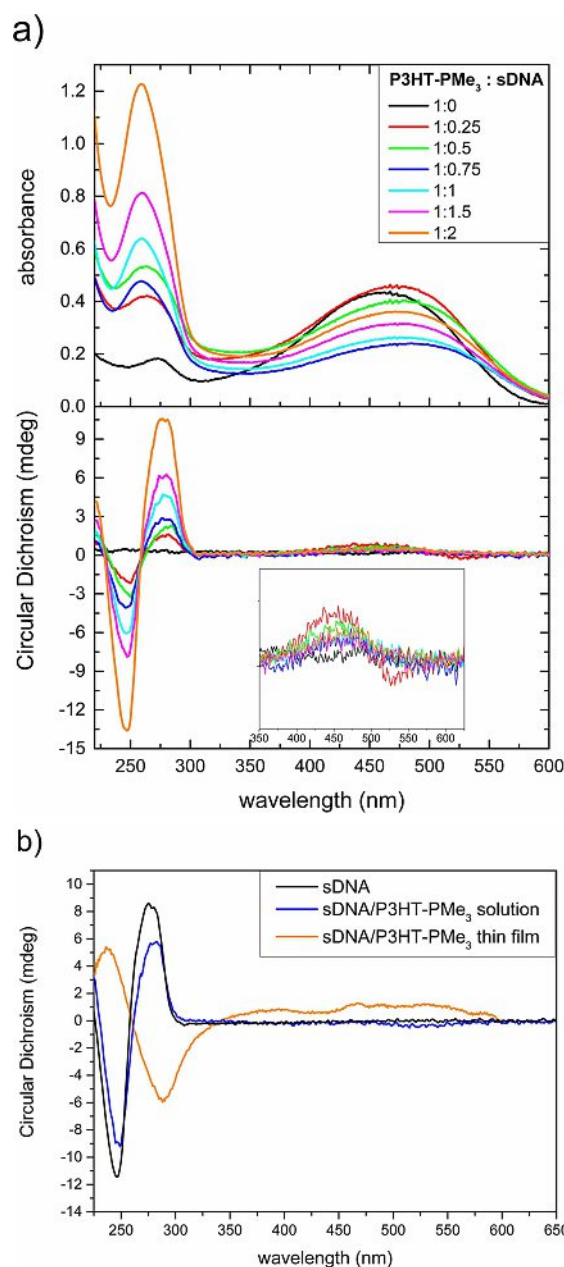


Figure 3. a) UV-vis (top) and CD (bottom) spectra of $P3HT-PMe_3$ titration by $sDNA$ in monomer (m)/base pairs (bp) ratio. $[P3HT-PMe_3]_m = 330 \mu M$ constant during the experiment. Inset: zoom of the CD spectra in the range 350–625 nm. b) CD spectra of $sDNA$ (black line), $sDNA/P3HT-PMe_3$ complex (blue line) in solutions (at a 1:1 DNA/polymer charge ratio) and the solid state CD spectrum of thin films of $sDNA/P3HT-PMe_3$ (orange line) at charge ratio 1:3.

Microscopic Morphology of Polyplexes on Surfaces

To further investigate possible hierarchical self-assembly processes of the polyplexes on surfaces, we studied thin deposits of the mixture solution by microscopy techniques. Figure 4 shows Atomic Force Microscopy (AFM) images of thin deposits (made by soaking the mica substrate into solutions) of pure $P3HT-$

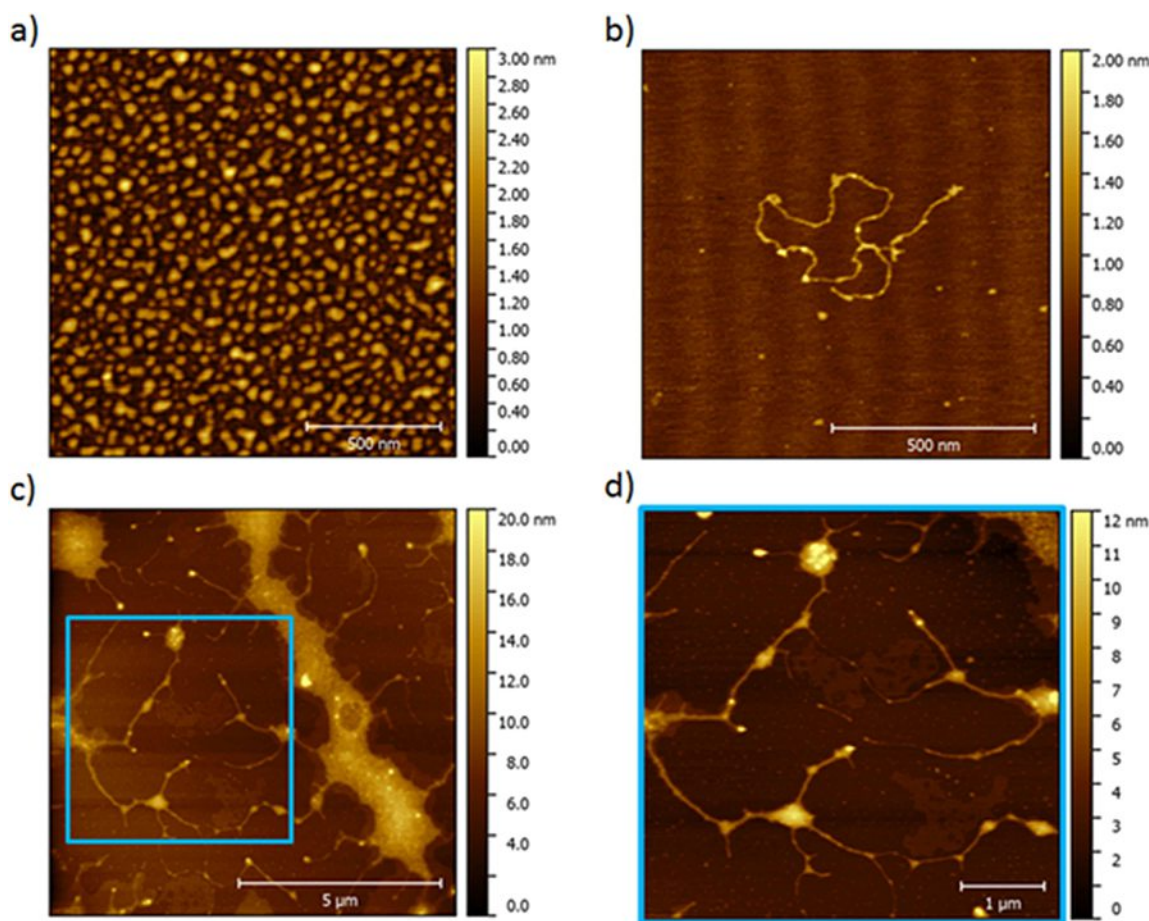


Figure 4. Tapping-Mode AFM images of thin deposits on mica of solutions of: a) pure P3HT-PMe₃; b) pure sDNA, and (c,d) sDNA/P3HT-PMe₃ complexes. Image in d) corresponds to a zoom in the area marked by a blue square depicted in c).

PMe₃ (Figure 4a), pure sDNA (Figure 4b), and sDNA/p3HT-PMe₃ (Figure 4c–d) on a mica substrate (dry thin deposits). Figure 4a showed that the pure polymer forms as described previously,^[18] granular structures of varying sizes, with an average width of around 0.1 μm and an average thickness of 1.7 nm. Thin deposits of pure sDNA showed the typical worm-like structures of DNA (Figure 4b). In contrast to the morphologies of pure compounds, thin deposits of sDNA/P3HT-PMe₃ exhibit a dendritic morphology (Figure 4c), *i.e.* tens of μm-long elongated aggregates with fiber-like branches (see zoom in Figure 4d) that extend over a few μm. In Figure 4c, the width and thickness of the main stem appearing in diagonal of the image are above 1 μm and around 8 nm, respectively. The branches at the periphery of this structure have a diameter ranging from 0.1 μm to 0.25 μm, and a thickness of 3 nm in average. The granular and flat structures present in between the dendrites (or branches) have an average height of around 1–2 nm, and are likely grains of uncomplexed P3HT-PMe₃, as observed for thin deposits of the pure polymer (see Figure 4a). Hence, the self-assembly of sDNA with P3HT-PMe₃ leads to an extended dendritic morphology with different levels of organization. These observations can be related to the works of Knaapila, Scherf, *et al.*, who studied the self-assembly of salmon DNA

with a π-conjugated copolymer containing a cationic polythiophene block, at various charge ratios.^[19] They showed that the self-assembly between the copolymer and DNA can yield fractal sub-micrometer-scaled structures, such as the dendritic morphology observed here. Note that the sharpest fibers on the Figure 3d have an average diameter around 30.0 nm ± 3 nm. This is to compare to the estimates of the R_h of around 25 nm in solution. It is likely that the fibers grow by compaction and coalescence of polyplexes along an axis during the deposit formation.

Confocal Optical Microscopy (COM) was used to visualise the sDNA/P3HT-PMe₃ complexes at a larger scale and to observe the fluorescence of the complexes when the samples are excited at 480 nm. Note here that the samples are studied at the solution/surface interface from a droplet deposited on a glass substrate. Figure 5a shows a large-scale image with many coiled fiber-like structures of different sizes (typically a few tens μm-long), which are reminiscent of the elongated μm-wide fiber-like aggregates observed with AFM. Since those fibers were observed in both types of AFM and COM analyses, this means that the self-assembly into fibers occurs at the solution/surface interface. A zoom showing the fluorescence image (excitation at 480 nm) of a particularly long fiber is shown in

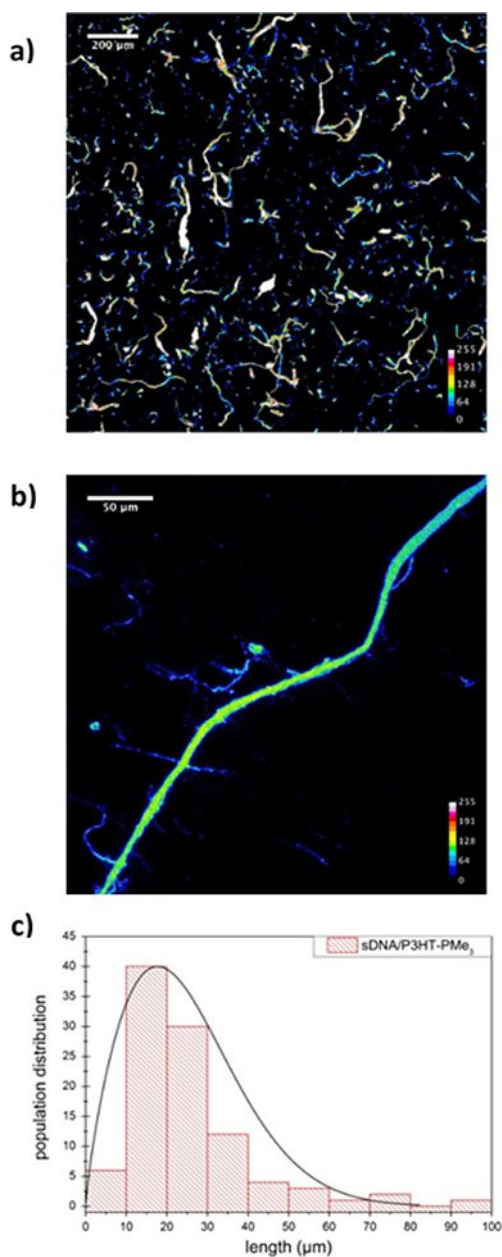


Figure 5. a), b) Confocal optical microscopy images of sDNA/P3HT-PMe₃ with the fluorescence intensity (colour scale). c) Size distribution of the fibers along their long axis. The excitation wavelength was 480 nm. The concentration of sDNA is 0.12 μM and the concentration of polymer is 5 μM.

Figure 5b, where the dendritic structure can be observed as with AFM. Strikingly, a relatively homogeneous fluorescence is noted on both the large fiber and smaller branches, which shows that the polymer is homogeneously complexed within the fibers. Based on the length distribution of the fibers (shown in Figure 5c for a population over a hundred fibers), we estimated the median being at 21 μm.

Both microscopy analyses showed us the evolution of the morphology going from the pure compounds to the morphology arising from the self-assembly of sDNA/P3HT-PMe₃, for which a dendritic structure is observed with large fibers

extending over tens of μm and thinner branched nanostructures at their periphery.

Altogether, these results bring new insights into the self-assembly of DNA with cationic polythiophenes in aqueous solution and on surfaces. The sizes of the polyplexes in solution are of a few nm in case of assemblies with short single-stranded DNA, and around 25 nm for longer DNA (sDNA) at a *N/P* ratio of 12, which are the typical sizes of polyplexes for applications in gene delivery. When the solution is deposited on a surface, we observed the formation of dendritic fibers, that can extend over tens of μm. Along these fibers, the π-conjugated polymer shows a relatively homogeneous luminescence, and the DNA is likely compacted in PSI-aggregate, as indicated by CD in the solid-state. Altogether, these results provide some guidelines towards the formation of DNA/CPT assemblies as polyplexes for prospective applications in cell transfection, or self-assembled fibers for organic bioelectronics.

Experimental Details

P3HT-PMe₃ (average molecular weight $M_n \sim 17,700 \text{ g mol}^{-1}$) was synthesized as reported earlier^[9] and dissolved in TE buffer (10 mM of Tris-HCl and 1 mM of EDTA). Salmon DNA samples were purchased from Aldrich and oligonucleotides were purchased from Eurogentec (Belgium) with the highest purity grade (>95% pure in sequence) in the dried state. DNA samples were dissolved in a volume of TE buffer (pH 7.4, 10 mM Tris buffer and 1 mM EDTA) at stock concentration of 170 μM for dT₂₀ and 0.6 μM (in strands) for sDNA of 170 μM. ODN solutions were centrifuged during 2 minutes at 2000 rpm. Typically, volumes of 20 μL of this solution were used to prepare different aliquots, to which were added TE buffer, and the final solution was mixed using a vortex. The exact concentration of DNA in the buffer solution was determined by UV-Vis absorption at 25 °C using the specific extinction coefficients at 260 nm (ϵ_{260}): 162600 L mol⁻¹ cm⁻¹ for dT₂₀ and 13200 L mol⁻¹ cm⁻¹ by base pairs (bp) for sDNA. The formation of DNA/P3HT-PMe₃ complexes was studied in TE buffer, mixing the P3HT-PMe₃ with each different DNA sample at vigorous speed for 1 minute and allowed to equilibrate for at least 10–15 minutes.

Spectroscopy. UV-Vis absorption and CD measurements were recorded using a Chirascan™ Plus CD Spectrometer from Applied Photophysics. The measurements were carried out using 2 mm suprasil quartz cells from Hellma Analytics. The spectra were recorded between 230 and 650 nm, with a bandwidth of 1 nm, time per point 0.5 s and two repetitions. The buffered water solvent reference spectra were used as baselines and were automatically subtracted from the CD spectra of the samples. For the CD spectra in solid state, a droplet of solution was deposited on a quartz suprasil plate and we let the sample dry. The solid-state study was carried out using a Chirascan CD integrating sphere with a high diffuse reflection factor, increasing the number of light beams to the CD detector. For microscopy studies, the sample solutions were the same as for spectroscopic studies.

Microscopy. Samples for AFM imaging were produced as follows: freshly-cleaved mica substrates were used and sunk into the solution during 5 to 10 min. The samples were then removed from the solution and washed with Milli-Q water, and then dried with a gentle nitrogen flow. The AFM analyses were carried out in Tapping-Mode in air at room temperature using a Nanoscope III from Bruker, using NCHV tips ($f_0 = 320 \text{ KHz}$) from Bruker probes. Confocal optical microscopy images were carried out by placing

droplets of solutions images were taken with a 1024×1024 pixels resolution (length and width images = 1640 μm).

Formation of polyplexes. Polyplexes were prepared directly before TDA experiments. A 0.116 g/L double-stranded salmon DNA (sDNA) solution and a 4.5 g/L P3HT-PMe₃ polycation solution were prepared in TE buffer (10 mM TRIS-HCl, 1 mM EDTA at pH 7.4). A 30 μL aliquot of P3HT-PMe₃ solution was first added to 70 μL TE buffer solution. The resulting mixture was then added to a 100 μL sDNA solution and shortly stirred at room temperature. N/P molar ratio was 12. Similar procedure was applied to the oligonucleotides dT₂₀. A 0.85 g/L oligonucleotide solution and a 45 g/L P3HT-PMe₃ polycation solution were prepared in TE buffer. A 5 μL aliquot of P3HT-PMe₃ solution was added to a mixture composed of 250 μL dT₂₀ solution and 45 μL TE buffer solution. N/P molar ratio was 1. A 50 μL aliquot of P3HT-PMe₃ solution was added to a 250 μL dT₂₀ solution. N/P molar ratio was 10. The resulting mixtures were briefly stirred at room temperature. In all cases, polyplexes were allowed to equilibrate for 30 min before analysis by TDA.

Taylor Dispersion Analysis experiments (TDA). Capillaries were prepared from bare silica tubing purchased from Polymicro Technologies (Photon Lines, Saint-Germain-en-Lay, France). All TDA experiments were carried out at 25 °C using frontal mode (i.e. by continuous injection of the sample). Each sample is prepared in the background electrolyte (TE buffer: 10 mM TRIS-HCl, 1 mM EDTA, pH 7.4). Before sample analysis, the capillary was previously filled with the same buffer. All TDA experiments were performed in triplicates.

TDA experiments were performed on a P/ACE MDQ system (Beckman, USA) using 50 μm i.d. × 40 cm (30 cm to the detector) capillaries. Capillaries were coated with poly(diallyl dimethyl ammonium chloride) (PDADMAC, M_w = 500,000 g/mol). For that, the capillaries were first conditioned with 1 M NaOH for 20 min and water for 5 min, then flushed with a 0.2% PDADMAC aqueous solution for 10 min, and finally flushed with TE buffer for 10 min. TDA experiments were carried out using 30 mbar mobilization pressure. Solutes were monitored by UV absorbance at 214 nm.

To increase the detection sensitivity, TDA was implemented in frontal mode, meaning that the sample is continuously and hydrodynamically injected into the capillary,^[13] leading to the detection of a front instead of a peak. For a bimodal mixture composed of two populations of different sizes, the temporal signal front is given by:

$$S(t) = \frac{S_1 + S_2}{2} + \frac{S_1}{2} \operatorname{erf}\left(\frac{t - t_0}{\sigma_1 \sqrt{2}}\right) + \frac{S_2}{2} \operatorname{erf}\left(\frac{t - t_0}{\sigma_2 \sqrt{2}}\right) \quad (1)$$

where t_0 is the average elution time, σ_1 and σ_2 are the square roots of the temporal variance of the two contributions in the elution profile, and S_1 and S_2 are two constants that depend on the response factor and injected quantity of the two populations present in the solute.

Equation (1) is valid provided that t_0 is much longer than the characteristic diffusion time of the solute in the cross section of the capillary ($t_0 \geq 1.25R_c^2/D$ for a relative error ϵ on the determination of D lower than 3%) and that the axial diffusion is negligible compared to convection (the Peclet number $Pe = R_c u/D$ is above 40 for ϵ lower than 3%, with u being the average linear mobile phase velocity)^[20]

The hydrodynamic radii R_h of the two species are related to their corresponding σ^2 according to:

$$R_h = \frac{k_b T}{6\pi\eta D} = \frac{4\sigma^2 k_b T}{\pi\eta R_c^2 t_0} \quad (2)$$

where k_b is the Boltzmann constant, T is the temperature (in K), R_c is the capillary diameter, and η is the viscosity of the eluent (0.9×10^{-3} Pa.s for TE buffer).

In this work, DNA (sDNA or dT₂₀) and P3HT-PMe₃ polycation were considered as substrate (S) and ligand (L), respectively. Polyplex SL_n are composed of one substrate S and n ligands (L), where n is the stoichiometry of the polyplex which is given by:

$$\bar{n} = \frac{[L]_0 - [L]}{[S]_0} \quad (3)$$

where $[L]_0$ and $[S]_0$ are the initial introduced concentrations of the ligand and the substrate, respectively, and $[L]$ is the free polycation (ligand) concentration. $[L]$ is obtained from the signal contribution due to the free ligand by external calibration (see SI for the calibration curve).

Acknowledgements

This work was supported by the Fonds de la Recherche Scientifique-FNRS (Belgium) under the grants n°1.B333.15F (CHIRNATES) and n°F.4532.16 (MIS-SHERPA). J.R.-M. and M.S. are FNRS researchers. The authors also thank CNRS and the University of Montpellier for financial support.

Conflict of Interest

The authors declare no conflict of interest.

Keywords: supramolecular self-assembly · DNA · cationic polythiophene · polyplexes · fibers

- [1] a) E. Busseron, Y. Ruff, E. Moulin, N. Giuseppone, *Nanoscale* **2013**, *5*, 7098–7140; b) *Supramolecular Systems in Biomedical Fields*, Ed. H.-J. Schneider, RSC Publishing, Cambridge, **2013**; c) J. Boekhoven, S. I. Stupp, *Adv. Mater.* **2014**, *26*, 1642–1659; d) M. Kumar, P. Brocorens, C. Tonnelé, D. Beljonne, M. Surin, S. J. George, *Nat. Commun.* **2014**, *5*, 5793; e) M. Palma, J. G. Hardy, G. Tadayyon, M. Farsari, S. J. Wind, M. J. Biggs, *Adv. Healthc. Mater.* **2015**, *4*, 2500–2519.
- [2] a) Y. Ruff, T. Moyer, C. J. Newcomb, B. Demeler, S. I. Stupp, *J. Am. Chem. Soc.* **2013**, *135*, 6211–6219; b) N. Stephanopoulos, R. Freeman, H. A. North, S. Sur, S. J. Jeong, F. Tatakitti, J. A. Kessler, S. I. Stupp, *Nano Lett.* **2015**, *15*, 603–609; c) Y. Wang, K. S. Schanze, E. Y. Chi, D. G. Whitten, *Langmuir* **2013**, *29*, 10635–10647; d) S. L. Kuan, Y. Wu, T. Weil, *Macromol. Rapid Commun.* **2013**, *34*, 380–392; e) R. Freeman, N. Stephanopoulos, Z. Alvarez, J. A. Lewis, S. Sur, C. M. Serrano, J. Boekhoven, S. S. Lee, S. I. Stupp, *Nat. Commun.* **2017**, *8*, 15982.
- [3] a) B. Shi, M. Zheng, W. Tao, R. Chung, D. Jin, D. Ghaffari, O. C. Farokhzad, *Biomacromolecules* **2017**, *18*, 2231–2246; b) H. Tang, X. Duan, X. Feng, L. Liu, S. Wang, Y. Li, D. Zhu, *Chem. Commun.* **2009**, 641–643; c) C. K. McLaughlin, G. D. Hamblin, H. F. Sleiman, *Chem. Soc. Rev.* **2011**, *40*, 5647–5656.
- [4] a) B. S. Gaylord, A. J. Heeger, G. C. Bazan, *J. Am. Chem. Soc.* **2003**, *125*, 896–900; b) C. Chi, A. Mikhailovsky, G. C. Bazan, *J. Am. Chem. Soc.* **2007**, *129*, 11134–11145; c) H.-A. Ho, A. Najari, M. Leclerc, *Acc. Chem. Res.* **2008**, *41*, 168–178; d) P. Björk, D. Thomson, O. Mirzov, J. A. Wigenius, O. Inganäs, I. G. Scheblykin, *Small* **2009**, *5*, 96–103. e) C. Zhu, L. Liu, Q. Yang, F. Lv, S. Wang, *Chem. Rev.* **2012**, *112*, 4687–4735; f) F. Xia, X. Zuo, R. Yang, Y. Xiao, D. Kang, A. Vallée-Belisle, X. Gong, A. J. Heeger, K. W.

- Plaxco, *J. Am. Chem. Soc.* **2010**, *132*, 1252–1254; g) Z. Liu, H. L. Wang, M. Cotellet, *Chem. Commun.* **2014**, *50*, 11311–11313.
- [5] a) K. P. Nilsson, O. Inganäs, *Nat. Mater.* **2003**, *2*, 419–424; b) M. Hamed, A. Elfving, R. Gabrielsson, O. Inganäs, *Small* **2013**, *9*, 363–368; c) F. Wang, M. Li, B. Wang, J. Zhang, Y. Cheng, L. Liu, F. Lv, S. Wang, *Sci. Rep.* **2015**, *5*, 7617.
- [6] C. Zhang, J. Ji, X. Shi, X. Zheng, X. Wang, F. Feng, *ACS Appl. Mater. Interfaces* **2018**, *10*, 4519–4529.
- [7] Y. Zhang, X. Li, T. Wu, J. Sun, X. Wang, L. Cao, F. Feng, *ACS Appl. Mater. Interfaces* **2017**, *9*, 16735–16740.
- [8] G. Yang, H. Yuan, C. Zhu, L. Liu, Q. Yang, F. Lv, S. Wang, *ACS Appl. Mater. Interfaces* **2012**, *4*, 2334–2337.
- [9] J. Rubio-Magnieto, A. Thomas, S. Richeter, A. Mehdi, P. Dubois, R. Lazzaroni, S. Clément, M. Surin, *Chem. Commun.* **2013**, *49*, 5483–5485.
- [10] a) J. Rubio-Magnieto, E. G. Azene, J. Knoops, S. Knippenberg, C. Delcourt, A. Thomas, S. Richeter, A. Mehdi, P. Dubois, R. Lazzaroni, D. Beljonne, S. Clément, M. Surin, *Soft Matter* **2015**, *11*, 6460–6471; b) J. Knoops, J. Rubio-Magnieto, S. Richeter, S. Clément, M. Surin, in *Materials and Energy*, Vol. 9 (Ed.: M. Knaapila), World Scientific, **2018**, pp. 139–157.
- [11] U. Lächelt, E. Wagner, *Chem. Rev.* **2015**, *115*, 11043–11078.
- [12] H. C. J. Chamieh, *Size-based characterization of nanomaterials by Taylor dispersion analysis*, Chapter 9, Eds. H. Ohshima and K. Makino, Elsevier, Amsterdam (The Netherlands), **2014**.
- [13] H. Cottet, J. P. Biron, M. Martin, *Anal. Chem.* **2007**, *79*, 9066–9073.
- [14] S. R. L. Leclercq, J. Chamieh, E. Wagner, H. Cottet, *Macromolecules* **2015**, *48*, 7216–7221.
- [15] J. C. F. Lounis, P. Gonzalez, H. Cottet, L. Leclercq, *Macromolecules* **2016**, *49*, 3881–3888.
- [16] a) L. Zhang, M. Liu, *J. Phys. Chem. B* **2009**, *113*, 14015–14020. b) G. Pescitelli, L. Di Bari, N. Berova, *Chem. Soc. Rev.* **2014**, *43*, 5211–5233; c) M. Liu, L. Zhang, T. Wang, *Chem. Rev.* **2015**, *115*, 7304–7397.
- [17] a) V. A. Bloomfield, *Biopolymers* **1997**, *44*, 269–282; b) B. I. Kankia, V. Buckin, V. A. Bloomfield, *Nucleic Acids Res.* **2001**, *29*, 2795–2801.
- [18] J. E. Houston, M. Chevrier, M.-S. Appavou, S. M. King, S. Clément, R. C. Evans, *Nanoscale* **2017**, *9*, 17481–17493.
- [19] M. Knaapila, T. Costa, V. M. Garamus, M. Kraft, M. Drechsler, U. Scherf, H. D. Burrows, *Macromolecules* **2014**, *47*, 4017–4027.
- [20] H. Cottet, J. P. Biron, M. Martin, *Analyst* **2014**, *139*, 3552–3562.

Manuscript received: January 9, 2019

Accepted: January 28, 2019

Version of record online: February 22, 2019